Auger Recombination of Biexcitons and Negative and Positive Trions in Individual Quantum Dots

Young-Shin Park,[†] Wan Ki Bae,[†,‡] Jeffrey M. Pietryga,[†] and Victor I. Klimov[†,*]

[†]Chemistry Division, Los Alamos National Laboratory, Los Alamos, New Mexico 87545, United States, and [‡]Photo-Electronic Hybrid Research Center, Korea Institute of Science and Technology, Seoul 136-791, Korea

ABSTRACT Charged exciton states commonly occur both in spectroscopic studies of quantum dots (QDs) and during operation of QD-based devices. The extra charge added to the neutral exciton modifies its radiative decay rate and also opens an additional nonradiative pathway associated with an Auger process whereby the recombination energy of an exciton is transferred to the excess charge. Here we conduct single-dot spectroscopic studies of Auger recombination in thick-shell ("giant") CdSe/CdS QDs with and without an interfacial alloy layer using time-tagged, time-correlated single-photon counting. In photoluminescence (PL) intensity trajectories of some of the dots, we resolve three distinct states of different emissivities ("bright", "gray", and "dark") attributed, respectively, to the neutral exciton and negative and positive trions. Simultaneously acquired PL lifetime trajectories indicate that the positive trion is much shorter lived than the negative trion, which can be explained by a high density of valence band states and a small hole localization radius (defined by the QD core size), factors that favor an Auger process involving intraband excitation of a hole. A comparison of trion and biexciton lifetimes suggests that the biexciton Auger decay can be treated in terms of a superposition of two independent channels associated with positive- and negative-trion pathways. The resulting interdependence between Auger time constants might simplify the studies of multicarrier recombination by allowing one, for example, to infer Auger lifetimes of trions of one sign based on the measurements of biexciton decay and dynamics of the trions of the opposite sign or, alternatively, estimate the biexciton lifetime based on studies of trion dynamics.

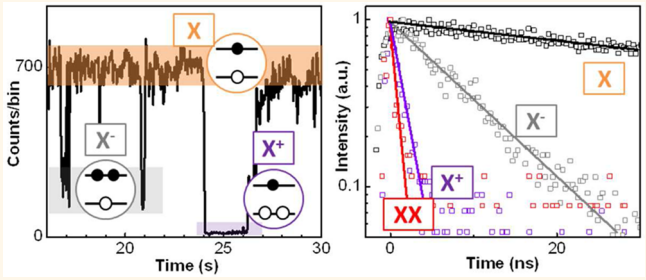

KEYWORDS: semiconductor nanocrystal · quantum dot · neutral exciton · charged exciton · trion · biexciton · Auger recombination · single-dot spectroscopy

Auger recombination is a nonradiative multicarrier process whereby the electron–hole recombination energy is not converted into a photon but instead transferred to a third charge.[1] Auger decay is extremely efficient in quantum dots (QDs) due to both close proximity between interacting charges and the relaxation of momentum conservation, leading to extremely fast dynamics on time scales from a few to hundreds of picoseconds depending on QD size.[2−8] Photoluminescence (PL) quenching by nonradiative Auger processes complicates realization of applications that require high emissivity of multicarrier states, such as light-emitting diodes (LEDs),[9−12] lasers,[13] and single-photon or photon-pair sources.[14,15] In particular, recent studies of QD-LEDs indicate that even a slight imbalance between electron and hole injection currents can lead to charging of the QD emitting layer, which lowers the external quantum efficiency and leads to an earlier onset of the efficiency roll-off due to increased nonradiative losses *via* Auger recombination in charged QDs.[11,16]

Previous experimental studies of Auger decay have mostly focused on charge-neutral multiexcitons such as biexcitons and triexcitons.[2,3,8,17−21] They established several important trends that govern this process in nanocrystals of various complexities including spherical or nearly spherical QDs,[2,21] elongated nanorods,[22,23] and core–shell heterostructures.[17,24,25] One such universal trend is a direct scaling of multiexciton Auger lifetimes with nanocrystal volume (sometimes referred to as "*V*-scaling")

* Address correspondence to klimov@lanl.gov.

Received for review April 29, 2014 and accepted June 8, 2014.

Published online June 09, 2014
10.1021/nn5023473

originally discovered in studies of CdSe QDs[2] and later observed for standard monocomponent QDs of many other compositions including direct and indirect gap semiconductors.[6]

Auger dynamics of charged species have been less thoroughly investigated partially due to difficulties in controlling the degree of charging. Approaches to creating a well-defined charged state include electrochemical charge injection[26,27] or chemical treatments with reducing or oxidizing species.[28−30] With a lesser degree of control, charged states can also be created during excitation with energetic electrons[31] or photoexcitation. In the latter case, uncompensated charges can be generated by a variety of processes including Auger ionization,[32−34] hot-electron transfer[35,36] to a surface trap, or tunneling of photoexcited charges to a proximal metal or semiconductor.[37,38]

The simplest charged state is a trion. It comprises a neutral exciton and either an extra electron (negative trion, X^-; Figure 1a) or an extra hole (positive trion, X^+; Figure 1b). In an idealized structure with identical conduction and valence bands, the Auger lifetimes of negative (τ_{A,X^-}) and positive (τ_{A,X^+}) trions are equal to each other and, further, are 4 times longer than the neutral biexciton Auger lifetime ($\tau_{A,XX}$). Indeed, based on "statistical" arguments,[4,39] the biexciton Auger decay can be described in terms of a superposition of two independent positive-trion- and negative-trion-like pathways (Figure 1c), implying that its rate can be presented as

$$1/\tau_{A,XX} = 2(1/\tau_{A,X^-} + 1/\tau_{A,X^+}) \quad (1)$$

which leads to $\tau_{A,X^-} = \tau_{A,X^+} = 4\tau_{A,XX}$ if we assume that $\tau_{A,X^-} = \tau_{A,X^+}$.

Recent studies of Auger decay in negatively charged PbSe QDs that feature nearly mirror symmetric conduction and valence bands seem to confirm this relationship.[29] Specifically, the measured Auger lifetime of the negative trion (τ_{A,X^-} = 360 ps) was almost 4 times longer than that of a neutral biexciton ($\tau_{A,XX}$ = 104 ps). On the other hand, significant deviations from this relationship have been observed for standard CdSe QDs[7] as well as core/shell CdSe/ZnSe[31] and CdSe/CdS QDs.[18] These measurements typically indicate that the X^- Auger lifetime is longer than $4\tau_{A,XX}$, which suggests that τ_{A,X^-} is not equal to but is in fact longer than τ_{A,X^+} (Figure 1d,e). An apparent exception to this trend was presented in a recent study of core/shell CdTe/CdSe QDs.[40] According to this work the negative-trion Auger lifetime could be almost equal to that of a biexciton, which questions the validity of eq 1 at least as applied to some of the QD materials.

Here, to elucidate the relationship between negative- and positive-trion Auger lifetimes, and further, their connection to the biexciton Auger lifetime, we conduct single-dot studies of carrier dynamics in thick-shell "giant" CdSe/CdS QDs (g-QDs) with and without intentional alloying of the core/shell interface. In order to address the issue of the validity of eq 1, we conduct independent evaluation of all three Auger times constants τ_{A,X^-}, τ_{A,X^+}, and $\tau_{A,XX}$ as derived from the analysis of PL intensity and lifetime trajectories measured using time-tagged time-correlated single-photon counting (TCSPC). We observe that while the majority of the g-QDs exhibit stable, nonblinking PL, some of the dots show fluctuation between either two or three states of different emissivities. On the basis of the analysis of intensities and lifetimes of these states we assign them to neutral excitons and negative and positive trions. In contrast to the ideal situation when τ_{A,X^+} is equal to τ_{A,X^-}, our measurements indicate that τ_{A,X^-} is considerably longer than τ_{A,X^+} in these QDs. The observed disparity between negative- and positive-trion lifetimes can be explained by a greater spectral density of valence- *vs* conduction-band states and a much smaller effective localization radius of a hole compared to that of an electron; both of these factors increase the relative efficiency of the positive- *vs* negative-trion Auger pathway. Interestingly, even in the case of a very large difference between τ_{A,X^-} and τ_{A,X^+}, the biexciton Auger lifetimes can be still accurately described by eq 1, supporting the validity of considering biexciton Auger decay in QDs as a superposition of independent (that is, uncorrelated) negative- and positive-trion pathways.

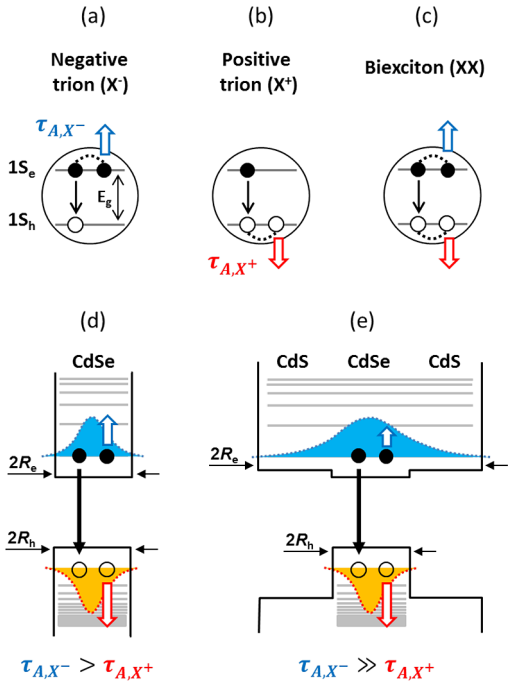

Figure 1. Schematic description of nonradiative Auger recombination of (a) a negative trion (X^-), (b) a positive trion (X^+), and (c) a biexciton (XX); E_g is the band gap energy. Asymmetry between X^- and X^+ Auger recombination pathways in (d) CdSe core-only and (e) thick-shell CdSe/CdS QDs.

RESULTS AND DISCUSSION

While Auger decay of negative trions has been the subject of several studies,[7,18,40,41] the dynamics of positive trions in QDs still remain poorly characterized. Without such characterization, however, one cannot evaluate the relationship between biexciton lifetimes and the lifetimes of negative and positive trions and thus assess the validity of eq 1. Only recently have all three time constants been measured for $CuInSe_xS_{2-x}$ QDs[42] in a study conducted in the context of their application in liquid-junction solar cells.[43,44] This work indicated a significant disparity between X^- and X^+ time constants (τ_{A,X^-} = 230 ps and τ_{A,X^+} = 60 ps). Nevertheless, the measured biexciton lifetime (25 ps) was close to that calculated using eq 1, that is, assuming contributions from independent X^+ and X^- pathways, which yielded 24 ps. The above results were obtained using a complex set of measurements on samples prepared as both QD solutions (used for XX and X^- measurements) and QDs incorporated into mesoporous titania, which served as an electron scavenger (X^+ measurements). Here, we demonstrate that in the case of thick-shell CdSe/CdS QDs we can avoid these complexities and extract all three time constants (τ_{A,X^-}, τ_{A,X^+}, and $\tau_{A,XX}$) from a single time-tagged TCSPC measurement conducted on individual QDs. Furthermore, from the same measurement we also obtain relative emission quantum yields (QYs) of X^- and X^+ and then compare them to those estimated from the measured time constants, which allows us to evaluate the relationship between radiative decay rates of neutral and charged excitons.

Samples for single-dot measurements were prepared on glass substrates by drop-casting from a dilute hexane QD solution. Pulsed radiation from a 488 nm diode laser (~40 ps pulse width, repetition rate v = 1 MHz) was focused onto the sample *via* an oil immersion objective lens (60×, 1.3 numerical aperture-), which was also used for collecting emission from individual QDs. PL photons, split between the two channels using a Hanbury Brown and Twiss setup, were detected with two single-photon avalanche photodiodes (time resolution ~350 ps) and processed with standard TCSPC electronics (PicoQuant). In these measurements, we utilized a multichannel, time-tagged, time-resolved mode, which allowed us to simultaneously record a PL intensity trajectory, PL decay dynamics of both single excitons and biexcitons,[45] and a second-order intensity correlation function; the latter was used to evaluate the degree of photon antibunching and thus ensure that the measurements were conducted on single QDs.[17] In all experiments, the entire PL spectrum without any spectral filtering was collected and analyzed. All measurements were conducted using low excitation intensities when the average number of photons absorbed per dot per pulse, $\langle N \rangle$, was less than 1 (typically, $\langle N \rangle$ was *ca.* 0.1). Given that in our QDs the longest time constant of the population decay (defined by the single exciton lifetime τ_X) was within 60−90 ns (see below), this excitation regime satisfied the condition $v\langle N \rangle < 1/\tau_X$, which prevented "excitation pile-up" over multiple pump pulses and thus ensured that the average QD occupancy was much smaller than 1.

In the present study we have examined two types of thick-shell CdSe/CdS QDs that differ in the properties of the core/shell interface.[11] One type features an abrupt boundary between the CdSe core and CdS shell, achieved by using a fast shell-growth method that avoids interfacial alloying. The other type has a compositionally graded interface, obtained by incorporating a thin intermediate layer of a $CdSe_xSe_{1-x}$ alloy, which reduces the rate of Auger recombination.[18,45,46] We will refer to these structures as core/shell (C/S) and core/alloy/shell (C/A/S) QDs, respectively. In both types of QDs the electron wave function is delocalized over the entire QD, whereas the hole remains largely confined to the core (Figure 1e), which corresponds to a so-called quasi-type-II localization regime.[47] A large difference in the effective localization radii of the electron and the hole leads to reduced electron−hole overlap, which is manifested in an increased exciton radiative lifetime ($\tau_{r,X}$) compared to core-only QDs.[48]

The C/S QDs studied here feature a CdSe core radius (r) of 1.5 nm and a CdS shell thickness (H) of 5.5 nm. The C/A/S QDs have the same overall radius (R = 7 mm); however, immediately outside of the 1.5 nm CdSe core, they contain a 1.5 nm thick alloyed layer ($CdSe_xS_{1-x}$ with x of *ca.* 0.5). The majority of the dots (>70%) from these samples featured essentially nonblinking PL (that is, stayed "on" for at least 90% of the time of the measurement; see Supporting Information, Sections 3 and 4) with no apparent switching to lower emissivity states. Here, we focus on a smaller fraction (~10%) of dots that exhibited pronounced PL intermittency.

Previous studies of PL blinking in thick-shell g-QDs have been interpreted in terms of switching between the neutral (X) and negatively charged (X^-) exciton states.[26,34,49,50] In dots where Auger decay of X^- is not completely suppressed, this switching results in variations of both PL intensity and lifetime.[26,49] On the other hand, in QDs with a considerable suppression of Auger recombination ($\tau_{A,X^-} > \tau_{r,X^-}$; τ_{r,X^-} is the X^- radiative lifetime), charge fluctuations lead only to a fluctuating PL lifetime without considerable changes in PL intensity. This regime was termed "lifetime blinking".[34]

In the present measurements, for some of the "blinking" dots we were able to resolve not just two but three states of different emissivities. These behaviors are illustrated in Figure 2, where we display PL intensity trajectories, intensity histograms, and decay dynamics measured for a C/S QD (Figure 2a,b,c) and a C/A/S QD (Figure 2d,e,f). As usual, the high-emissivity

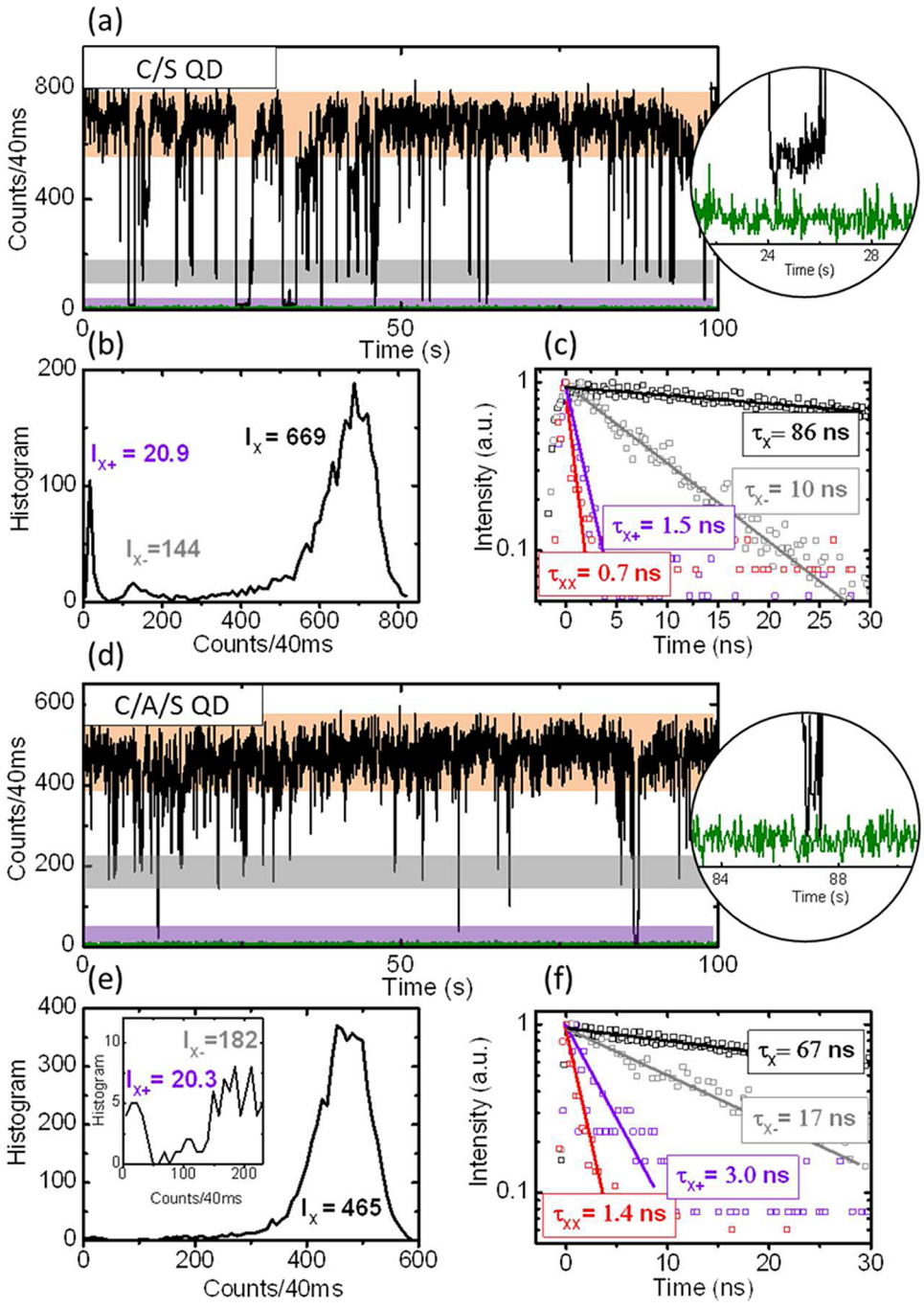

Figure 2. PL intensity trajectories (a, d), histograms (b, e), and dynamics (c, f) measured for individual C/S CdSe/CdS (a−c) and C/A/S CdSe/CdSeS/CdS (d−f) QDs. Both QDs have the same core radius (r = 1.5 nm) and the same total radius (R = 7.0 nm); the C/A/S QD has an intermediate alloyed layer with thickness L = 1.5 nm. Three distinct states with different emissivities are shown in (a) and (d) by different shadings: orange ("bright" state), gray ("gray" state), and purple ("dark" state); these states correspond, respectively, to neutral exciton and negative and positive trions. Their dynamics are shown in (c) and (f) using the same color coding; the biexciton dynamics included in these plots are shown in red. Insets in (a) and (d) show a magnified view of portions of intensity trajectories assigned to X^+ emission; corresponding intensities are well above the background level. Inset in (e) is a magnified view of a portion of the PL intensity histogram, which corresponds to charged excitons (X^- and X^+).

"bright" state can be assigned to a neutral exciton. As we show below, the characteristics of the two lower emissivity states are consistent with those of the negative (intermediate PL intensity level; "gray" state) and positive (lowest PL intensity level; "dark" state) trions. We would like to point out that the average photon count rate for the "dark" states (>400 counts/s) was well above the background level (~130 counts/s, green lines in the insets of Figures 2a,d; see also Supporting Information, Section 1).

In Figure 2c,f, we plot decay curves obtained by recording arrival times of PL photons from the three different intensity bands of the single-dot PL trajectory that correspond to "bright (orange shading), "gray"

(gray shading), and "dark" (purple shading) states. For the C/S QD (Figure 2c), an exponential fit yields the "bright" state lifetime τ_b = 86 ns. The lifetimes of the "gray" and "dark" states are, correspondingly, τ_g = 10 ns and τ_d = 1.5 ns. If these states are indeed associated with negative and positive trions, the expected biexciton Auger lifetime would be 0.69 ns. This value is estimated using eq 1 by taking into account both Auger and radiative decay channels (that is, $1/\tau_{X^-(X^+)} = 1/\tau_{r,X^-(X^+)} + 1/\tau_{A,X^-(X^+)}$) and assuming that the trion radiative rate can be calculated from $\tau_{r,X^-(X^+)} = \tau_{r,X}/2$ = 43 ns.[45] A direct single-QD measurement of biexciton dynamics (see Methods) yields τ_{XX} = 0.70 ns, from which we can estimate a biexciton Auger decay time constant $\tau_{A,XX}$ = 0.72 ns assuming that the biexciton radiative lifetime $\tau_{r,XX} = \tau_{r,X}/4$ = 21.5 ns. This value is in a good agreement with the estimation based on the measured dynamics of the "gray" and "dark" states (0.69 ns), suggesting that these states indeed correspond to X^- and X^+, respectively. Previously, low-emissivity periods due to positive trions with a comparable lifetime (*ca.* 1 to 2 ns) were observed in single-dot spectroelectrochemical studies of CdSe/CdS QDs (Supplementary Figure 2 of ref 26).

The analysis of the intensity trajectories and PL dynamics for a single C/A/S QD (Figures 2d,e,f) indicates a similar lifetime of the "bright" neutral exciton state ($\tau_b = \tau_X$ = 67 ns). On the other hand, the lifetimes of charged X^- and X^+ states ($\tau_g = \tau_{X^-}$ = 17 ns and $\tau_d = \tau_{X^+}$ = 3.0 ns) are about a factor of 2 longer than in the C/S QD. This is an expected result of core/shell potential grading leading to suppression of Auger recombination[46] as was first observed for g-QDs with unintentionally alloyed core/shell interfaces[24] and later in dots with deliberate interfacial alloying used to explore the concept of "interface engineering" for improving the performance of QD-LEDs.[11]

On the basis of the time constants measured for the C/A/S QD, trion Auger lifetimes are τ_{A,X^-} = 34.5 ns and τ_{A,X^+} = 3.3 ns, *versus*, respectively, 13 and 1.6 ns in C/S QDs. Direct single-dot measurements of the XX dynamics indicate that $\tau_{A,XX}$ in the C/A/S QD is also approximately twice as long as in the C/S QD (1.4 ns *vs* 0.72 ns). However, even though Auger recombination is modified by grading of the core/shell potential, the rates of trion and biexciton recombination are still interdependent and can be related to each other by eq 1. Indeed, on the basis of the trion lifetimes the biexciton Auger lifetime estimated from eq 1 is 1.5 ns, that is, nearly the same as the measured value (1.4 ns). This agreement, systematically observed for all QDs with resolvable "gray" and "dark" emission levels (Figure 3a), confirms the validity of eq 1, which describes biexciton decay in terms of independent X^- and X^+ pathways and, furthermore, supports the interpretation of the "gray" and "dark" states in terms of, respectively, negative and positive trions. More examples of single-QD measurements that exhibit distinct three-state emissions are presented in Section 2 of the Supporting Information.

Earlier in this article, we used the typical assumption that radiative decay rates of multicarrier states can be related to that of a neutral exciton by "statistical" scaling,[51] which suggests that biexciton and trion radiative lifetimes are, respectively, 4 and 2 times shorter than $\tau_{r,X}$: $\tau_{r,XX} = \tau_{r,X}/4$ and $\tau_{r,X^+(X^-)} = \tau_{r,X}/2$. Using the results of single-dot measurements we can verify the validity of this assumption (at least, as applied to thick-shell g-QDs) by analyzing PL QYs of the X^+ and X^- states and their relation to the measured trion and neutral exciton lifetimes. The ratio of the trion and neutral exciton PL QYs can be derived from the ratio of their average intensities ($I_{X^+(X^-)}$ and I_X, respectively) using histograms of occurrences of different PL levels (Figures 2b,e): $Q_{X^+(X^-)}/Q_X = I_{X^+(X^-)}/I_X$. On the other hand, PL QYs can be found from the measured X^- (X^+) and X lifetimes: $Q_{X^+(X^-)}/Q_X = (\tau_{X^+(X^-)}/\tau_{r,X^+(X^-)}) \cdot (\tau_X/\tau_{r,X})^{-1}$. If we denote the ratio between radiative decay rates of a trion and a neutral exciton as β, the latter expression can be rewritten as $Q_{X^+(X^-)}/Q_X = \beta\tau_{X^+(X^-)}/\tau_X$. In the ideal case of statistical scaling, β = 2.

To determine the experimental values of parameter β, we first analyze the results for negative trions. In Figure 3b, we plot Q_{X^-}/Q_X as a function of the ratio of the trion and neutral exciton lifetimes and fit the experimental data to a linear dependence. On the basis of this procedure, we obtain that for negative trions β = 1.71 (C/S QDs) and 1.43 (C/A/S QDs). Both of these values are smaller than for the ideal statistical scaling. This discrepancy can be rationalized if we take into account excitonic effects, that is, the electron–hole Coulombic attraction. If electron–hole interaction is neglected, the electron is delocalized over an entire volume of the CdSe/CdS QD. However, in the presence of electrostatic interactions the electron becomes localized in the near-core region due to Coulomb potential of the core-localized hole.[52] The resulting state is analogous to a donor in bulk CdS, which is characterized by a radius of 2.6 nm and a binding energy of 32.7 meV.[53] The latter value is greater than thermal carrier energies at room temperature, implying that the donor-like exciton is a stable room-temperature state in g-QDs. The second electron introduced into the QD experiences effective repulsion from the QD core due to shielding of the hole potential by the negatively charged "cloud" of the first (core-bound) electron. This reduces the electron–hole overlap for the unbound electron and explains the reduction of β compared to its ideal value of 2.

The situation is, however, different for positive trions. If a hole is added to the neutral exciton, a large energy gradient defined by the valence band energy offset (~0.42 eV for CdSe/CdS QDs) leads to its localization in the CdSe core, regardless of any (much smaller) Coulombic interactions. Thus, the electron–hole

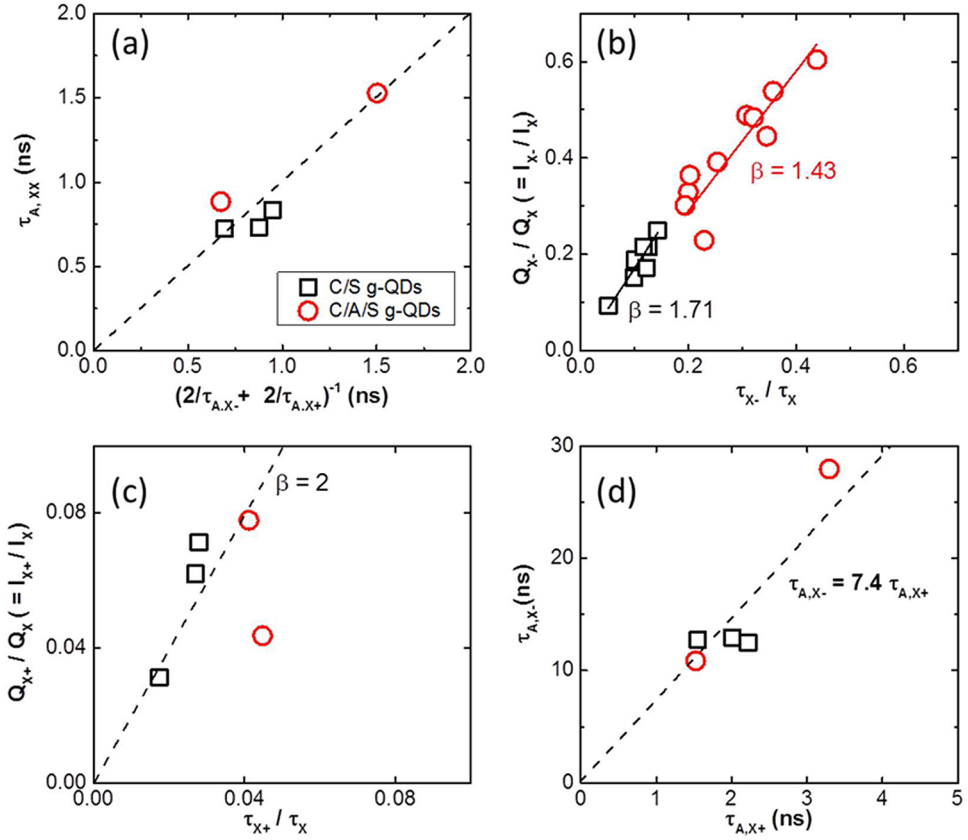

Figure 3. (a) Comparison of biexciton Auger lifetimes obtained in two different ways: a direct measurement of XX dynamics (shown on the vertical axis) *vs* estimations based on eq 1 using the measured trion lifetimes (shown on the horizontal axis); experimental data are close to the "ideal" dependence (dashed line) when the biexciton Auger decay rate is twice the sum of the X^- and X^+ Auger decay rates. Black squares and red circles correspond to the C/S and C/A/S samples, respectively. (b) PL quantum yields of a negative trion derived from PL intensity histograms plotted as a function of the X^- lifetime normalized by the neutral exciton lifetime; lines are linear dependencies with two different slopes (indicated in the figure). (c) Same for a positive trion. (d) Plot of τ_{A,X^-} as a function of τ_{A,X^+} shows a significant disparity between negative- and positive-trion lifetimes.

overlaps are identical for the two core-confined holes. As a result, the ratio of the radiative decay rates of X^+ and X is expected to be close to the ideal value of 2. Indeed, as illustrated in Figure 2c, for the majority of the QDs with the resolvable third emission level ("dark" state) the parameter β derived from the analysis of Q_{X^+} and τ_{X^+} is around 2.

The deviation of β from the ideal value of 2 observed for negative trions does not considerably affect the derivation of Auger lifetimes of biexcitons and specifically the data shown in Figure 3a for which the resulting correction is less than 1%. The corrections to trion Auger lifetimes due to a "nonideal" β is greater and can reach ~20% for X^-. Therefore, we re-evaluate Auger time constants of negative and positive trions using experimentally measured values of β and present these data in Figure 3d in the form of the τ_{A,X^-} *vs* τ_{A,X^+} plot. In the case when the X^+ and X^- Auger pathways are symmetric (as, for example, in PbSe QDs[29]), the data plotted in this way should reside near the diagonal line that corresponds to $\tau_{A,X^-} = \tau_{A,X^+}$. However, we find that for the studied g-QDs, the experimental lifetimes are close to the line with the slope of 7.4, indicating that τ_{A,X^-} is considerably longer than τ_{A,X^+}. The disparity between X^- and X^+ decay pathways in CdSe-based structures has been suggested by the results of several previous studies that indicated that X^- Auger lifetimes were longer than 4 times the biexciton Auger lifetime.[18] For example, cathodoluminescence measurements of XX and X^- dynamics[31] indicated that in standard thin-shell CdSe/ZnS QDs the ratio of τ_{A,X^-} and $\tau_{A,XX}$ could be as large as 6. On the basis of eq 1 this would suggest that the $\tau_{A,X^-}/\tau_{A,X^+}$ ratio is ~2.

To explain the disparity between the X^- and X^+ Auger decay pathways in CdSe-based QDs, one can invoke a strong asymmetry between the valence and conduction bands typical of II–VI semiconductors. Specifically, because of the multiband character of the valence band and large hole effective masses, the density of hole states in these materials is considerably higher than the density of electron states. As a result, in II–VI QDs the electron levels are much more widely separated than hole states. Indeed, it was previously

shown[54] that even near the band-edge the hole states in CdSe QDs can be described in terms of a dense quasi-continuum, and the density of hole states further increases with increasing energy. Due to this structure of electronic states, the energy conservation requirement is easier to meet for Auger processes involving intraband excitation of a hole *vs* those accompanied by excitation of an electron (Figure 1d). This favors the positive- *vs* negative-trion Auger pathway, which can explain the disparity between the τ_{A,X^-} and τ_{A,X^+} time constants observed in standard core-only and thin-shell CdSe QDs.

A dissimilarity between the localization radii of an electron and a hole that is characteristic of thick-shell CdSe/CdS g-QDs is expected to further enhance the difference between the X^- and X^+ Auger decay constants. Direct measurements of biexciton dynamics indicate that the rate of XX Auger recombination can be expressed as twice the sum of the X^- and X^+ Auger decay rates, suggesting that the biexciton decay can be treated in terms of a superposition of independent negative and positive trion pathways. As illustrated in Figure 1e, these two recombination channels can be described in terms of Coulombic scattering between the two electrons and the two holes, respectively. A smaller separation between holes (confined to core) *vs* the separation between the electrons (delocalized over the entire QD) is expected to lead to a relative enhancement of the positive- *vs* negative-trion decay pathway. This additional factor is likely responsible for a significant deviation from unity of the $\tau_{A,X^-}/\tau_{A,X^+}$ ratio observed in our measurements of thick-shell C/S and C/A/S samples (Figure 3d).

CONCLUSIONS

To summarize, we have performed single-dot spectroscopic studies of the Auger decay of charged excitons and biexcitons in C/S CdSe/CdS and C/A/S CdSe/CdSeS/CdS g-QDs. Neutral excitons and negative and positive trions were observed in intensity trajectories as states with respectively high, intermediate, and low emissivity levels, which allowed us to extract their characteristic decay constants from a single measurement conducted in a time-resolved time-tagged mode. In contrast to the ideal situation where the negative and positive trions have the same Auger lifetimes, we observe that τ_{A,X^-} is significantly longer than τ_{A,X^+} (by up to a factor of ~10). This disparity between τ_{A,X^-} and τ_{A,X^+} can be attributed to two factors: (1) a high spectral density of valence-band states, which favors the processes involving intraband excitation of a hole (that is, X^+ *vs* X^- Auger pathway) and (2) a smaller localization radius of holes (confined to the CdSe core) than electrons (delocalized over the entire hetero-QD), which increases the relative probability of hole–hole scattering events responsible for the X^+ Auger decay. Direct measurements of biexciton dynamics indicate that the rate of XX Auger recombination can be expressed as twice the sum of the X^- and X^+ Auger decay rates, suggesting that the biexciton decay can be treated in terms of a superposition of independent negative and positive trion Auger pathways.

METHODS

Decay dynamics of X, X^-, X^+, and XX were measured using a two-channel, time-tagged, time-resolved TCSPC module (PicoQuant) in conjunction with a Hanbury Brown and Twiss setup. PL decay curves of X, X^-, and X^+ were constructed by plotting the histograms of microtimes (time relative to a laser pulse) of photons that fall into intensity bands of respectively "bright", "gray", and "dark" states of the PL intensity trajectory. In order to obtain the biexciton decay constant, we considered the events of two-photon registration (one on each detector) for the same excitation laser pulse. By comparing microtimes of these two photons, the photon that arrives first was assigned to a biexciton, while the second to a single exciton.

Conflict of Interest: The authors declare no competing financial interest.

Supporting Information Available: Examination of background in PL measurements, additional examples of single QD emission with three emissivity levels, examples of nonblinking PL and two-state blinking, and the probability of detecting a "bright" neutral exciton state. This material is available free of charge *via* the Internet at http://pubs.acs.org.

Acknowledgment. This work was supported by the Chemical Sciences, Biosciences and Geosciences Division of Office of Science, Office of Basic Energy Sciences, U.S. Department of Energy.

REFERENCES AND NOTES

1. Landsberg, P. T. *Basic Properties of Semiconductors*; Elsevier Science Publishers, 1992.
2. Klimov, V. I.; Mikhailovsky, A. A.; McBranch, D. W.; Leatherdale, C. A.; Bawendi, M. G. Quantization of Multiparticle Auger Rates in Semiconductor Quantum Dots. *Science* **2000**, *287*, 1011–1013.
3. Pandey, A.; Guyot-Sionnest, P. Multicarrier Recombination in Colloidal Quantum Dots. *J. Chem. Phys.* **2007**, *127*, 111104.
4. Klimov, V. I. Multicarrier Interactions in Semiconductor Nanocrystals in Relation to the Phenomena of Auger Recombination and Carrier Multiplication. *Annu. Rev. Condens. Matter Phys.* **2014**, *5*, 285–316.
5. Pietryga, J. M.; Zhuravlev, K. K.; Whitehead, M.; Klimov, V. I.; Schaller, R. D. Evidence for Barrierless Auger Recombination in PbSe Nanocrystals: A Pressure-Dependent Study of Transient Optical Absorption. *Phys. Rev. Lett.* **2008**, *101*, 217401.
6. Robel, I.; Gresback, R.; Kortshagen, U.; Schaller, R. D.; Klimov, V. I. Universal Size-Dependent Trend in Auger Recombination in Direct-Gap and Indirect-Gap Semiconductor Nanocrystals. *Phys. Rev. Lett.* **2009**, *102*, 177404.
7. Jha, P. P.; Guyot-Sionnest, P. Trion Decay in Colloidal Quantum Dots. *ACS Nano* **2009**, *3*, 1011–1015.
8. Fisher, B.; Caruge, J.-M.; Chan, Y.-T.; Halpert, J.; Bawendi, M. G. Multiexciton Fluorescence from Semiconductor Nanocrystals. *Chem. Phys.* **2005**, *318*, 71–81.
9. Mashford, B. S.; Stevenson, M.; Popovic, Z.; Hamilton, C.; Zhou, Z.; Breen, C.; Steckel, J.; Bulovic, V.; Bawendi, M.;

Coe-Sullivan, S.; *et al*. High-Efficiency Quantum-Dot Light-Emitting Devices with Enhanced Charge Injection. *Nat. Photonics* **2013**, *7*, 407–412.
10. Colvin, V. L.; Schlamp, M. C.; Alivisatos, A. P. Light-Emitting Diodes Made from Cadmium Selenide Nanocrystals and a Semiconducting Polymer. *Nature* **1994**, *370*, 354–357.
11. Bae, W. K.; Park, Y.-S.; Lim, J.; Lee, D.; Padilha, L. A.; McDaniel, H.; Robel, I.; Lee, C.; Pietryga, J. M.; Klimov, V. I. Controlling the Influence of Auger Recombination on the Performance of Quantum-Dot Light-Emitting Diodes. *Nat. Commun.* **2013**, *4*.
12. Dabbousi, B. O.; Bawendi, M. G.; Onitsuka, O.; Rubner, M. F. Electroluminescence from CdSe Quantum-Dot/Polymer Composites. *Appl. Phys. Lett.* **1995**, *66*, 1316–1318.
13. Klimov, V. I.; Mikhailovsky, A. A.; Xu, S.; Malko, A.; Hollingsworth, J. A.; Leatherdale, C. A.; Eisler, H.-J.; Bawendi, M. G. Optical Gain and Stimulated Emission in Nanocrystal Quantum Dots. *Science* **2000**, *290*, 314–317.
14. Michler, P.; Imamoglu, A.; Mason, M. D.; Carson, P. J.; Strouse, G. F.; Buratto, S. K. Quantum Correlation Among Photons from a Single Quantum Dot at Room Temperature. *Nature* **2000**, *406*, 968–970.
15. Lounis, B.; Bechtel, H. A.; Gerion, D.; Alivisatos, P.; Moerner, W. E. Photon Antibunching in Single CdSe/ZnS Quantum Dot Fluorescence. *Chem. Phys. Lett.* **2000**, *329*, 399–404.
16. Bae, W. K.; Brovelli, S.; Klimov, V. I. Spectroscopic Insights into the Performance of Quantum Dot Light-Emitting Diodes. *MRS Bull.* **2013**, *38*, 721–730.
17. Park, Y.-S.; Malko, A. V.; Vela, J.; Chen, Y.; Ghosh, Y.; García-Santamaría, F.; Hollingsworth, J. A.; Klimov, V. I.; Htoon, H. Near-Unity Quantum Yields of Biexciton Emission from CdSe/CdS Nanocrystals Measured Using Single-Particle Spectroscopy. *Phys. Rev. Lett.* **2011**, *106*, 187401.
18. Bae, W. K.; Padilha, L. A.; Park, Y.-S.; McDaniel, H.; Robel, I.; Pietryga, J. M.; Klimov, V. I. Controlled Alloying of the Core−Shell Interface in CdSe/CdS Quantum Dots for Suppression of Auger Recombination. *ACS Nano* **2013**, *7*, 3411–3419.
19. Beard, M. C.; Knutsen, K. P.; Yu, P.; Luther, J. M.; Song, Q.; Metzger, W. K.; Ellingson, R. J.; Nozik, A. J. Multiple Exciton Generation in Colloidal Silicon Nanocrystals. *Nano Lett.* **2007**, *7*, 2506–2512.
20. Kraus, R. M.; Lagoudakis, P. G.; Müller, J.; Rogach, A. L.; Lupton, J. M.; Feldmann, J.; Talapin, D. V.; Weller, H. Interplay between Auger and Ionization Processes in Nanocrystal Quantum Dots. *J. Phys. Chem. B* **2005**, *109*, 18214–18217.
21. Zhao, J.; Nair, G.; Fisher, B. R.; Bawendi, M. G. Challenge to the Charging Model of Semiconductor-Nanocrystal Fluorescence Intermittency from Off-State Quantum Yields and Multiexciton Blinking. *Phys. Rev. Lett.* **2010**, *104*, 157403.
22. Zavelani-Rossi, M.; Lupo, M. G.; Tassone, F.; Manna, L.; Lanzani, G. Suppression of Biexciton Auger Recombination in CdSe/CdS Dot/Rods: Role of the Electronic Structure in the Carrier Dynamics. *Nano Lett.* **2010**, *10*, 3142–3150.
23. Htoon, H.; Hollingsworth, J. A.; Dickerson, R.; Klimov, V. I. Effect of Zero- to One-Dimensional Transformation on Multiparticle Auger Recombination in Semiconductor Quantum Rods. *Phys. Rev. Lett.* **2003**, *91*, 227401.
24. García-Santamaría, F.; Chen, Y.; Vela, J.; Schaller, R. D.; Hollingsworth, J. A.; Klimov, V. I. Suppressed Auger Recombination in "Giant" Nanocrystals Boosts Optical Gain Performance. *Nano Lett.* **2009**, *9*, 3482–3488.
25. Oron, D.; Kazes, M.; Banin, U. Multiexcitons in Type-II Colloidal Semiconductor Quantum Dots. *Phys. Rev. B* **2007**, *75*, 035330.
26. Galland, C.; Ghosh, Y.; Steinbruck, A.; Sykora, M.; Hollingsworth, J. A.; Klimov, V. I.; Htoon, H. Two Types of Luminescence Blinking Revealed by Spectroelectrochemistry of Single Quantum Dots. *Nature* **2011**, *479*, 203–207.
27. Wehrenberg, B. L.; Guyot-Sionnest, P. Electron and Hole Injection in PbSe Quantum Dot Films. *J. Am. Chem. Soc.* **2003**, *125*, 7806–7807.
28. Shim, M.; Guyot-Sionnest, P. Organic-Capped ZnO Nanocrystals: Synthesis and n-Type Character. *J. Am. Chem. Soc.* **2001**, *123*, 11651–11654.
29. Koh, W.-k.; Koposov, A. Y.; Stewart, J. T.; Pal, B. N.; Robel, I.; Pietryga, J. M.; Klimov, V. I. Heavily Doped n-type PbSe and PbS Nanocrystals Using Ground-State Charge Transfer from Cobaltocene. *Sci. Rep.* **2013**, *3*.
30. Engel, J. H.; Surendranath, Y.; Alivisatos, A. P. Controlled Chemical Doping of Semiconductor Nanocrystals Using Redox Buffers. *J. Am. Chem. Soc.* **2012**, *134*, 13200–13203.
31. Padilha, L. A.; Bae, W. K.; Klimov, V. I.; Pietryga, J. M.; Schaller, R. D. Response of Semiconductor Nanocrystals to Extremely Energetic Excitation. *Nano Lett.* **2013**, *13*, 925–932.
32. Klimov, V. I.; McBranch, D. W. Auger-Process-Induced Charge Separation in Semiconductor Nanocrystals. *Phys. Rev. B* **1997**, *55*, 13173–13179.
33. Peterson, J. J.; Nesbitt, D. J. Modified Power Law Behavior in Quantum Dot Blinking: A Novel Role for Biexcitons and Auger Ionization. *Nano Lett.* **2008**, *9*, 338–345.
34. Galland, C.; Ghosh, Y.; Steinbrück, A.; Hollingsworth, J. A.; Htoon, H.; Klimov, V. I. Lifetime Blinking in Nonblinking Nanocrystal Quantum Dots. *Nat. Commun.* **2012**, *3*, 908.
35. McGuire, J. A.; Sykora, M.; Robel, I.; Padilha, L. A.; Joo, J.; Pietryga, J. M.; Klimov, V. I. Spectroscopic Signatures of Photocharging due to Hot-Carrier Transfer in Solutions of Semiconductor Nanocrystals under Low-Intensity Ultraviolet Excitation. *ACS Nano* **2010**, *4*, 6087–6097.
36. Padilha, L. A.; Robel, I.; Lee, D. C.; Nagpal, P.; Pietryga, J. M.; Klimov, V. I. Spectral Dependence of Nanocrystal Photoionization Probability: The Role of Hot-Carrier Transfer. *ACS Nano* **2011**, *5*, 5045–5055.
37. Krauss, T. D.; Brus, L. E. Charge, Polarizability, and Photoionization of Single Semiconductor Nanocrystals. *Phys. Rev. Lett.* **1999**, *83*, 4840–4843.
38. Li, S.; Steigerwald, M. L.; Brus, L. E. Surface States in the Photoionization of High-Quality CdSe Core/Shell Nanocrystals. *ACS Nano* **2009**, *3*, 1267–1273.
39. Klimov, V. I.; McGuire, J. A.; Schaller, R. D.; Rupasov, V. I. Scaling of Multiexciton Lifetimes in Semiconductor Nanocrystals. *Phys. Rev. B* **2008**, *77*, 195324.
40. Qin, W.; Liu, H.; Guyot-Sionnest, P. Small Bright Charged Colloidal Quantum Dots. *ACS Nano* **2013**, *8*, 283–291.
41. Cohn, A. W.; Rinehart, J. D.; Schimpf, A. M.; Weaver, A. L.; Gamelin, D. R. Size Dependence of Negative Trion Auger Recombination in Photodoped CdSe Nanocrystals. *Nano Lett.* **2013**, *14*, 353–358.
42. Makarov, N. S.; McDaniel, H.; Fuke, N.; Robel, I.; Klimov, V. I. Photocharging Artifacts in Measurements of Electron Transfer in Quantum-Dot-Sensitized Mesoporous Titania Films. *J. Phys. Chem. Lett.* **2013**, *5*, 111–118.
43. McDaniel, H.; Fuke, N.; Pietryga, J. M.; Klimov, V. I. Engineered $CuInSe_xS_{2-x}$ Quantum Dots for Sensitized Solar Cells. *J. Phys. Chem. Lett.* **2013**, *4*, 355–361.
44. McDaniel, H.; Fuke, N.; Makarov, N. S.; Pietryga, J. M.; Klimov, V. I. An Integrated Approach to Realizing High-Performance Liquid-Junction Quantum Dot Sensitized Solar Cells. *Nat. Commun.* **2013**, 4.
45. Park, Y.-S.; Bae, W. K.; Padilha, L. A.; Pietryga, J. M.; Klimov, V. I. Effect of the Core/Shell Interface on Auger Recombination Evaluated by Single-Quantum-Dot Spectroscopy. *Nano Lett.* **2014**, *14*, 396–402.
46. Cragg, G. E.; Efros, A. L. Suppression of Auger Processes in Confined Structures. *Nano Lett.* **2009**, *10*, 313–317.
47. Piryatinski, A.; Ivanov, S. A.; Tretiak, S.; Klimov, V. I. Effect of Quantum and Dielectric Confinement on the Exciton−Exciton Interaction Energy in Type II Core/Shell Semiconductor Nanocrystals. *Nano Lett.* **2006**, *7*, 108–115.
48. Brovelli, S.; Schaller, R. D.; Crooker, S. A.; García-Santamaría, F.; Chen, Y.; Viswanatha, R.; Hollingsworth, J. A.; Htoon, H.; Klimov, V. I. Nano-Engineered Electron−Hole Exchange Interaction Controls Exciton Dynamics in Core−Shell Semiconductor Nanocrystals. *Nat. Commun.* **2011**, *2*, 280.
49. Spinicelli, P.; Buil, S.; Quélin, X.; Mahler, B.; Dubertret, B.; Hermier, J. P. Bright and Grey States in CdSe-CdS

Nanocrystals Exhibiting Strongly Reduced Blinking. *Phys. Rev. Lett.* **2009**, *102*, 136801.
50. Malko, A. V.; Park, Y.-S.; Sampat, S.; Galland, C.; Vela, J.; Chen, Y.; Hollingsworth, J. A.; Klimov, V. I.; Htoon, H. Pump-Intensity- and Shell-Thickness-Dependent Evolution of Photoluminescence Blinking in Individual Core/Shell CdSe/CdS Nanocrystals. *Nano Lett.* **2011**, *11*, 5213–5218.
51. McGuire, J. A.; Joo, J.; Pietryga, J. M.; Schaller, R. D.; Klimov, V. I. New Aspects of Carrier Multiplication in Semiconductor Nanocrystals. *Acc. Chem. Res.* **2008**, *41*, 1810–1819.
52. Shabaev, A.; Rodina, A. V.; Efros, A. L. Fine Structure of the Band-Edge Excitons and Trions in CdSe/CdS Core/Shell Nanocrystals. *Phys. Rev. B* **2012**, *86*, 205311.
53. Henry, C. H.; Nassau, K. Magneto-Optical Studies of Excited States of the Cl Donor in CdS. *Phys. Rev. B* **1970**, *2*, 997–1004.
54. Htoon, H.; Cox, P. J.; Klimov, V. I. Structure of Excited-State Transitions of Individual Semiconductor Nanocrystals Probed by Photoluminescence Excitation Spectroscopy. *Phys. Rev. Lett.* **2004**, *93*, 187402.